Titin-induced force enhancement and force depression: A 'sticky-spring' mechanism in muscle contractions?

Christian Rode, Tobias Siebert, Reinhard Blickhan

www.elsevier.com/locate/yjtbi

Titin-induced force enhancement and force depression: A 'sticky-spring' mechanism in muscle contractions?

Christian Rode, Tobias Siebert, Reinhard Blickhan

PII: S0022-5193(09)00114-3
DOI: doi:10.1016/j.jtbi.2009.03.015
Reference: YJTBI 5490

To appear in: *Journal of Theoretical Biology*

Received date: 12 December 2008
Revised date: 2 March 2009
Accepted date: 4 March 2009

Cite this article as: Christian Rode, Tobias Siebert and Reinhard Blickhan, Titin-induced force enhancement and force depression: A 'sticky-spring' mechanism in muscle contractions?, *Journal of Theoretical Biology* (2009), doi:10.1016/j.jtbi.2009.03.015

Titin-induced force enhancement and force depression: A 'sticky-spring' mechanism in muscle contractions?

Christian Rode*, Tobias Siebert and Reinhard Blickhan

Institute of Motion Science, Friedrich Schiller University,

Seidelstr. 20, 07749 Jena, Germany

*Corresponding author, christian.rode@uni-jena.de,

Tel.: 0049 3641 945704, Fax: 0049 3641 945702

The sliding filament and crossbridge theories do not suffice to explain a number of muscle experiments. For example, from the entire muscle to myofibrils, predictions of these theories were shown to underestimate the force output during and after active tissue stretch. The converse applies to active tissue shortening.

In addition to the crossbridge cycle, we propose that another molecular mechanism is effective in sarcomere force generation. We suggest that, when due to activation, myosin binding sites are available on actin, the giant protein titin's PEVK region attaches itself to the actin filament at those sites. As a result, the molecular spring length is dramatically reduced. This leads to increased passive force when the sarcomere is stretched and to decreased or even negative passive force when the sarcomere shortens. Moreover, during shortening, the proposed mechanism interferes with active-force production by inhibiting crossbridges.

Incorporation of a simple 'sticky-spring' mechanism model into a Hill-type model of sarcomere dynamics offers explanations for several force-enhancement and force-depression effects. For example, the increase of the sarcomere force compared to the force predicted solely by the sliding filament and crossbridge theories depends on the stretch amplitude and on the working range. The same

applies to the decrease of sarcomere force during and after shortening. Using only literature data for its parameterization, the model predicts forces similar to experimental results.

Key words: molecular mechanism, model, stretch, shortening, sarcomere, myofilament interaction

1. Introduction

From whole muscle to myofibrils, the steady-state force after an active stretch can exceed the force measured in an isometric contraction at the same final length (Abbott and Aubert, 1952; Edman et al., 1982) and can even exceed the maximum isometric force (Herzog et al., 2008; Lee and Herzog, 2008). While the first result might be explained with non-uniform sarcomere lengthening (Morgan, 1990), the latter cannot be explained solely within the framework of the sliding filament (Huxley and Niedergerke, 1954; Huxley and Hanson, 1954) and the crossbridge theories (Huxley, 1957). The physiological mechanism(s) underlying enhanced forces have not been understood to date (see Herzog et al., 2008 for a review). However, it has been suggested that residual force enhancement (the force difference between the two measured steady-state forces) can be separated into active and passive parts (Herzog et al., 2006) related to the crossbridge mechanism and to titin, respectively (Herzog et al., 2008). In contrast, Pinniger et al. (2006) provided evidence suggesting that force enhancement during and after stretch results from a mechanism independent of the crossbridges and may be related to titin.

Stretching active fibers from the same initial length (throughout the manuscript initial refers to the length at which activation occurs) with different constant velocities, Edman et al. (1982) found constant stiffness greater than zero after a short transient

phase, suggesting a spring-like characteristic (elongation-dependent) of force enhancement. Moreover, muscles stretched on the descending limb of the active force-length relationship exceeded the isometric force at the stretched length by a larger amount than muscles stretched the same distance on the ascending limb (Morgan et al., 2000; Peterson et al., 2004). These effects are hard to explain with enhanced crossbridge forces. Not only would the crossbridge have to exert force rising with stretch amplitude, but it would also have to 'know' about the initial filament overlap. This substantiates the presence of a force-producing mechanism independent of the crossbridge force-generation producing increasing forces with increasing initial sarcomere length.

Another reported phenomenon of muscular contraction is the decreased steady-state force after active muscle (e.g. Abbott and Aubert, 1952) or fiber (e.g. Edman, 1975, 1996; Edman et al., 1993; Sugi and Tsuchiya, 1988) shortening compared to the force measured in an isometric contraction at the same final length. Residual force depression (force difference between these two measured steady state forces) was found to be proportional to the shortening distance (Marechal and Plaghki, 1979; Edman, 1975; Herzog and Leonard, 1997). Mechanisms proposed in this context include stress-induced inhibition of crossbridges (Marechal and Plaghki, 1979).

Physiological explanations, as well as most phenomenological descriptions, deal with either force enhancement (the increase in experimental force compared to the force expected from valid sliding filament and crossbridge theories; e.g. Morgan et al., 1982) or with force depression (the converse of the above; e.g. Marechal and Plaghki, 1979; Meijer et al., 1998). Forcinito et al. (1998) showed that a physiologically non-motivated recruitable elastic rack conceptually explains force enhancement and force depression effects. However, in contradiction to experimental results (Herzog and Leonard, 2000), such modeling predicts commutativity of shortening-stretch vs. stretch-shortening experiments with respect to the subsequent steady-state muscle force.

In this study, we propose and model a physiological mechanism related to titin (connectin) to describe both force-enhancement and force-depression effects. The giant protein titin is a structural part of myosin with a free part acting as a molecular spring connecting myosin to the Z-disc near the actin filament (Linke et al., 1998; Prado et al. 2005). This molecular spring consists of three morphologically distinct regions: 1) the proximal Immunoglobulin (Ig) region connecting to the Z-disc, 2) the adjacent PEVK region (rich in proline (P), glutamic acid (E), valine (V) and lysine (K)), and 3) the distal Ig region attached to myosin. Interaction with actin seems possible when calcium is present (Kellermayer and Granzier, 1996) and the PEVK region can attach to the actin filament (Bianco et al., 2007). Such attachments may occur at myosin binding sites on actin (Niederlander et al., 2004). Here, we assume that the PEVK region attaches itself to the myosin binding sites on actin during activation (Fig. 1, top), thereby altering titin's behavior during subsequent length changes compared to passive length changes. This 'sticky-spring' mechanism might induce considerable forces during and after sarcomere stretch, as well as during and after sarcomere shortening.

By dramatically reducing titin's free spring length in the active state (i.e. when calcium concentration is high), the 'sticky-spring' mechanism may lead to 1) increased passive half-sarcomere force during and after active stretch and 2) decreased or even negative passive half-sarcomere force during and after active shortening. Moreover, during shortening, the proposed mechanism may interfere with active-force production by inhibiting crossbridges. Resultant, the mechanism might offer an explanation for several force-enhancement and force-depression effects including the non-commutativity (Herzog and Leonard, 2000) of those effects.

2. Methods

2.1 Model

We restricted our modeling to the half-sarcomere as the force-producing unit of the muscle (Fig. 1) and neglected elasticity in series to the crossbridges such as elasticity of the actin and myosin filaments. In addition, we normalized forces to the maximum isometric active force $F_{[im]}$ (throughout the manuscript, values subscripted with brackets were constant for at least one experiment) produced at optimal thin (actin) and thick (myosin) filament overlap and assumed that all forces would act along the myofilament axis.

The normalized half-sarcomere force f_{hs} equaled the sum of an active (crossbridges) component f_{act} and a passive (titin) component f_{pass}:

$$f_{hs} = F_{hs} / F_{[im]} = f_{act} + f_{pass} . \quad (1)$$

A common Hill-type separation approach matching the sliding filament and crossbridge theories defined the active force:

$$f_{act} = F_{act} / F_{[im]} = f_v(v_{hs}) \cdot f_l(l_{hs}, l_{hs[0]}) . \quad (2)$$

The f_v is a factor due to the force-velocity (Hill, 1938; Abbot and Aubert, 1952) relation (shortening: $f_v < 1$; stretch: $f_v > 1$) and depends on the half-sarcomere velocity v_{hs}. The f_l is a factor due to the force-length (Gordon et al., 1966) relation ($f_l \leq 1$). According to the sliding filament theory, f_l depends on the number of effective crossbridges. Moreover, on the steep part of the ascending limb of the active force-length relationship, it also assumedly depends on counteracting compressive forces. Following the proposed mechanism, however, f_l can be decreased due to inhibited crossbridges; it not only

depends on the half-sarcomere length $l_{hs,}$ but also on the initial half-sarcomere length $l_{hs[0]}$ (please see appendix A).

We modeled titin's molecular spring region as an elastic spring. In the passive state (calcium concentration is low, i.e. the sarcomere is deactivated), f_{pass} is a function of l_{hs}. In the active state (calcium concentration is high, i.e. the sarcomere is activated), the PEVK region attaches itself to the actin filament. Hence, titin's distal Ig region can be pulled not only in the same direction (Fig. 1, middle) as the crossbridges ($f_{pass} > 0$), but also in the opposite (Fig. 1, bottom) direction ($f_{pass} < 0$). Resultant, f_{pass} is a function of l_{hs} and $l_{hs[0]}$ as described in the next section.

We assumed that skinned myofibril passive tension is induced by titin (Linke et al., 1998). With a typical value of maximum active muscle tension of 20 N/cm^2, we translated measured myofibril tension (Linke et al., 1998) into normalized tension corresponding to normalized titin force. Further length data (Linke et al., 1998) yielded force-elongation data for the entire molecular spring and for the distal Ig and PEVK regions (Fig. 2). We used lookup tables and linearly interpolated desired values from these essentially nonlinear data which were extrapolated linearly when necessary.

2.2 The titin-induced 'sticky-spring' mechanism

Consider a rectangular adhesive tape stuck on a plain surface. It can bear high forces if pulled along its length axis away from its adherend (stretch), but is easily peeled off in the opposite direction (shortening). We suggest that titin's PEVK region may function similarly during muscular contraction.

Along its length, the PEVK region seems to be able to attach to the actin filament, to quickly reattach itself when the bond is broken, and moreover, the attachment may bear an average maximum force $F_{[am]}$ of 8 pN (Bianco et al., 2007). In the active state, we assume that PEVK-actin attachment occurs spontaneously when the PEVK region

154 approaches a myosin binding site on actin, and that the attachment can bear $F_{[am]}$ in any
155 direction (i.e. in our model in any of the two longitudinal half-sarcomere directions).

156 To normalize the force induced by the 'sticky-spring' mechanism, we related $F_{[am]}$
157 to $F_{[im]}$. With assumed 20 N/cm^2 maximum isometric active muscle tension and a 42 nm
158 distance between myosin filaments in the crystalline structure of skeletal muscle, the
159 maximum active force related to one myosin is 300 pN. Six titin molecules connect
160 each myosin filament to the Z-disc at the corresponding actin filaments. Hence the
161 maximum isometric force related to one titin molecule is 50 pN, and $F_{[am]}$ = 8 pN
162 corresponds to $f_{[am]}$ = 0.16 normalized maximum attachment force.
163
164 *2.2.1 Single active stretch*

165 First, assume a high calcium concentration and that the PEVK region is attached to
166 actin thereby dramatically reducing the free molecular spring length to the distal Ig
167 region length (Fig. 1, top). At the initial half-sarcomere length $l_{hs[0]}$, the initial passive
168 half-sarcomere force $f_{pass[0]}$ acts in the PEVK region as well as in the proximal and
169 distal Ig regions. However, no force pulls on the PEVK-actin attachments. When the
170 active sarcomere is stretched, the force in the distal Ig region increases due to a pull on
171 the most distal (nearest to myosin) PEVK-actin attachment. As soon as the increase in
172 force exceeds the normalized attachment force $f_{[am]}$, the attachment may break and
173 PEVK may reattach at the same binding site, thus reducing the PEVK chain length
174 between the two most distal PEVK-actin attachments and leading to an additional force
175 bearing of the second (from distal) attachment site. If the stretch continues, more and
176 more of the initial PEVK-actin attachments will bear force, and the elongating PEVK
177 region will approach additional binding sites (Fig. 1, middle). Hence, during the stretch,
178 the PEVK region may be seen as a 'sticky-spring', and its distal-end force f_{sticky} is the

sum of the constant $f_{pass[0]}$ (compare appendix B) and the cumulated force pulling on the PEVK-actin attachments f_{att_cum} (Fig. 1, middle). Hence

$$f_{pass} = f_{sticky} = f_{pass[0]} + f_{att\_cum} . \quad (3)$$

Note that the sum of these forces does not indicate simultaneous parallel action, but a sequential increase of passive force.

We derived a constant stiffness $k_{[sticky]}$ dependent on $l_{hs[0]}$ to characterize the increase in force due to 'sticky-spring' elongation (see appendix B). The half-sarcomere length change equals the sum of the PEVK region's elongation Δl_{PEVK} equaling Δl_{sticky} and the distal Ig region's elongation Δl_{dist_Ig} (Fig. 1, middle):

$$l_{hs} - l_{hs[0]} = \Delta l_{sticky} + \Delta l_{dist\_Ig} = f_{att\_cum} / k_{[sticky]}(l_{hs[0]}) + l_{dist\_Ig} - l_{dist\_Ig[0]} , \quad (4)$$

where l_{dist_Ig} is the length of the distal Ig region and $l_{dist\_Ig[0]}$ is its length attained under $f_{pass[0]}$.

2.2.2 Single active shortening

Here, we only consider the case where the initial passive force is lower than $f_{[am]}$ which, according to the used literature data, corresponds to half-sarcomere lengths below 1.66 µm (f_l = .31, descending limb of active force-length relation). Such lengths are exceeded only by a few muscles within their operating ranges (Burkholder and Lieber, 2001). Again, assume that the PEVK region is attached to actin (Fig. 1, top) and further, that the most distal PEVK-actin attachment coincides with the distal end of the PEVK region. The following shortening can be separated into three distinct length

ranges with 'sticky-spring' effects on active and passive half-sarcomere forces. In the first phase (Fig. 3, top), shortening leads to a stronger decrease in passive force compared to passive shortening since the molecular spring length is reduced to the length of the distal Ig region. Hence

$$l_{dist\_Ig} = l_{dist\_Ig[0]} - (l_{hs[0]} - l_{hs}) . \quad (5)$$

The 'sticky-spring' force equaling the passive force is then given by the force-length data of the distal Ig region. Note that the PEVK region is pre-stretched by $f_{pass[0]}$ before attaching itself to actin. Therefore, as f_{sticky} decreases to zero during shortening to the first shortening phase's final length $l_{hs[1]}$, the resulting force pulling on the most distal PEVK-actin attachment towards the Z-disc increases from zero to $f_{pass[0]}$.

During the second shortening phase (Fig. 3, middle), a passive tensile force counteracting the active force develops in the distal Ig region. Notably, it also pulls solely on the most distal PEVK-actin attachment towards the Z-disc. Consequently, the PEVK-actin attachments break consecutively whenever this force exceeds $f_{[break]} = f_{[am]} - f_{pass[0]}$. Since the mechanical energy expended to peel off the PEVK region during half-sarcomere shortening increased approximately with the square of the displacement (Fig. C.1B), we assumed the 'sticky-spring' peel-off force to increase linearly with half-sarcomere shortening $l_{hs[1]} - l_{hs}$ with a slope of $k_{[short\_2]}$ depending on $l_{hs[0]}$ (see appendix C):

$$f_{pass} = -f_{sticky} = -k_{[short\_2]}(l_{hs[0]}) \cdot (l_{hs[1]} - l_{hs}) . \quad (6)$$

The negative sign indicates that the 'sticky-spring' force opposes the active force f_{act}.

Myosin entering the range of the attached PEVK region at the length $l_{hs[1]}$ reduces the number of effective crossbridges, thereby decreasing active forces compared to the crossbridge and sliding filament theories. The f_l value decrease is defined by the region l_{block} (compare appendix A) where potential crossbridges are inhibited by the attached PEVK region (Fig. 3, middle):

$$l_{block} = \begin{cases} l_{hs[1]} - l_{hs} - \Delta x_{PEVK\_dist}, & x_{PEVK\_prox[0]} < l_{hs} - l_{[myosin]} \\ l_{hs[1]} - l_{hs} - \Delta x_{PEVK\_dist} - (x_{PEVK\_prox[0]} - (l_{hs} - l_{[myosin]})), & x_{PEVK\_prox[0]} \geq l_{hs} - l_{[myosin]} \end{cases} . \quad (7)$$

The proximal displacement of the attached PEVK region's distal end Δx_{PEVK_dist} (Fig. 3, middle) is given by

$$\Delta x_{PEVK\_dist} = \begin{cases} 0, & l_{hs[1]} - l_{hs} < l_{[dist\_Ig\_break]} \\ s(l_{hs[0]}) \cdot (l_{hs[1]} - l_{hs} - l_{[dist\_Ig\_break]}), & l_{hs[1]} - l_{hs} \geq l_{[dist\_Ig\_break]} \end{cases}, \quad (8)$$

where $s(l_{hs[0]})$ (see appendix C) is a gearing < 1 relating the length change of the half-sarcomere $l_{hs[1]} - l_{hs}$ offset by $l_{[dist\_Ig\_break]}$ (the length of the distal Ig region strained by $f_{[break]}$) to Δx_{PEVK_dist}. The constant length $x_{PEVK\_prox[0]}$ corresponds to the distance between the Z-disc and the proximal end of the PEVK region, and $l_{[myosin]}$ (0.8 µm) is the length of half a myosin molecule.

The third shortening phase (Fig. 3, bottom) begins when the distal Ig region's distal end passes the PEVK region's proximal end at the corresponding length $l_{hs[2]}$. In this situation the distal Ig region is pre-stretched to $l_{dist\_Ig[2]}$ with the force $f_{sticky[2]}$ ($< f_{[break]}$). We assume that during half-sarcomere shortening $l_{hs[2]} - l_{hs}$ the PEVK region attaches as described in section 2.2.1 and that similar equations apply, however, resulting here in passive force counteracting the active force. Remaining initial PEVK-actin attachments

continue to break consecutively during shortening, thus, contrary to stretch, no initial PEVK-actin attachments can be recruited permanently for force bearing of the 'sticky-spring'. Thus, 'sticky-spring' force only increases due to approaching new binding sites on actin at intervals $c_{[bind]}$ (0.038 μm), and $k_{[sticky]}$ equals $f_{[am]}/c_{[bind]}$ (compare Fig. B.1A). Neglecting the decrease in force distal to the first newly approached binding site due to its minor role in passive force generation, the passive force equals (compare Eq. (3))

$$f_{pass} = -f_{sticky} = -(f_{sticky[2]} + f_{att\_cum}). \quad (9)$$

The proximal displacement of the PEVK region's proximal end Δx_{PEVK_prox} (Fig. 3, bottom) is defined by $k_{[sticky]}$. Hence (compare Eq. (4)),

$$l_{hs[2]} - l_{hs} = \Delta x_{PEVK\_prox} + \Delta l_{dist\_Ig} = f_{att\_cum} / k_{[sticky]} + l_{dist\_Ig} - l_{dist\_Ig[2]}. \quad (10)$$

For simplicity, we assumed that the attached PEVK-region's distal end moved towards the Z-disc by half Δx_{PEVK_prox} until it reached the third-phase initial locus of the proximal PEVK end. Hence

$$l_{block} = \begin{cases} l_{block[2]} + .5 \cdot \Delta x_{PEVK\_prox}, & \Delta x_{PEVK\_prox} < 2 \cdot l_{block[2]} \\ \Delta x_{PEVK\_prox}, & \Delta x_{PEVK\_prox} \geq 2 \cdot l_{block[2]} \end{cases}, \quad (11)$$

where $l_{block[2]}$ corresponds to the length l_{block} at the end of the second shortening phase.

Results

The 'sticky-spring' mechanism as modeled is independent of stretch or shortening velocity. Consequently, we show forces during active stretch (Fig. 4) and during active shortening (Fig. 5) from different initial lengths in force vs. half-sarcomere length plots. The f_v value resulting from the force-velocity relation modulating the active half-sarcomere force component is, however, set to 1 (isometric condition). This approach enables the reading of force enhancement during stretch and force depression during shortening, as well as the reading of residual force enhancement and residual force depression at any half-sarcomere length.

'Sticky-spring' stiffness in stretch experiments increases with increasing initial half-sarcomere length (Fig. B.1A).

Discussion

In addition to the crossbridge cycle, we proposed a titin-induced molecular 'sticky-spring' mechanism to contribute to sarcomere force generation. When compared to passive half-sarcomere length changes, it increases passive force during and after active stretch (Fig. 4, top), and it produces decreased or negative passive force during and after active shortening (Fig. 5, top). Moreover, during shortening, the 'sticky-spring' mechanism interferes with active force production by inhibiting crossbridges (Fig. 5, middle). The mechanism accounts for many experimental observations concerning force-enhancement and force-depression effects leaving the sliding filament and the crossbridge theories intact (i.e. without increasing or decreasing the rate functions of attachment or detachment of myosin heads to actin). Notably, we used only experimental data from the literature to derive 'sticky-spring' forces.

Residual force enhancement and residual force depression depend on the muscle's working range. More precisely, no residual force enhancement (Edman et al., 1982; Morgan et al., 2000; Peterson et al., 2004) and no residual force depression (Gordon et

al., 1966; Morgan et al., 2000) were found in the steep range of the ascending limb of the active force-length relationship. Furthermore, residual force enhancement increased from the upper part of the ascending limb to longer lengths (e.g. Herzog et al., 2008; Lee and Herzog, 2008). Predictions of the 'sticky-spring' mechanism reflect these findings. There is no titin length change in the range of the steep part of the ascending limb of the active force-length relationship (myosin hits Z-disc), and thus neither residual force enhancement nor residual force depression are predicted for contractions within this length range. Predicted residual force enhancement increases from the upper part of the ascending limb to longer lengths (Fig. 4) due to increasing 'sticky-spring' stiffness (Fig. B.1A, inset).

Measured residual force depression D (Edman, 1975; 20 % for .15μm half-sarcomere shortening to plateau) is lower by an order of magnitude than residual force enhancement (Herzog et al., 2008; 170 % for .35μm half-sarcomere stretch from plateau). The 'sticky-spring' mechanism predictions are similar to these experimental results (Figs 4, 5).

Sarcomere lengths, though inhomogeneous before stretch, were shown to homogenize during and after stretch on the descending limb of the active force-length relationship (Herzog et al., 2008). Stunningly, this is contrary to what would be expected according to the sliding-filament and the crossbridge theories. The longer the sarcomere, the weaker it should be and should elongate more rapidly until it is 'caught' by passive forces at long lengths which is not seen in the cited experiments. In general, the 'sticky-spring' mechanism leads to higher passive forces during and after active stretch compared to during and after passive stretch. The higher passive stiffness in initially longer sarcomeres, and accordingly the higher passive force during and after stretch in those sarcomeres could result in a compensation of lower active forces

328 compared to initially shorter sarcomeres and lead to homogenization of sarcomere
329 lengths as observed.

330 For large magnitude stretches, residual force enhancement can reach a plateau
331 (Bullimore et al., 2007) whose development is within the framework of the proposed
332 mechanism. During a stretch, the force gradient in the PEVK region might reach the
333 proximal (to Z-disc) PEVK-region end. Further stretch would then lead to movement of
334 the entire PEVK region along actin at a rather constant force (neglecting the increase in
335 passive force in the proximal Ig region). The lower the bearable PEVK-actin attachment
336 force and the shorter and the stiffer the PEVK region, the lower the stretch magnitude at
337 which the plateau occurs and the lower the plateau force.

338 Moreover, residual force enhancement (Edman et al., 1982) as well as residual force
339 depression (Herzog and Leonard, 1997) do not disappear if force temporarily decreases
340 to zero during stretch or shortening, but vanish if activation temporarily decreases to
341 zero after the final stretch or shortening length is reached. With regards to the 'sticky-
342 spring' mechanism, this also makes perfect sense because it is independent of a decrease
343 in force to zero induced by a quick shortening step. On the other hand, when the
344 sarcomere deactivates, the PEVK-actin attachments must break according to our theory,
345 otherwise the proposed mechanism would be a one-way street. We expect tropomyosin
346 to break the PEVK-actin attachments while covering the myosin binding sites on actin.

347

348 *Model limitations*

349 Though many experimental results might be explained qualitatively with the mechanism
350 proposed in its current form, a well-documented feature of force depression is not yet
351 included. Similar to experiments by Marechal and Plaghki (1979), the 'sticky-spring'
352 mechanism leads to residual force depression which linearly depends on the shortening
353 distance in a number of ranges (Fig. 6). However, residual force depression not only

depends on shortening distance, but also on shortening velocity (Marechal and Plaghki, 1979).

Considering the narrow interfilamentary space, it may be possible that instead of sliding past them, the myosin filaments knock off a fraction of PEVK-actin attachments during shortening. The impulse exerted on the PEVK-actin attachment increases with increasing contraction velocity. Hence, the probability of knock-off might increase with velocity resulting in decreased force depression. To incorporate the speculated knock-off into the model in a simple manner, we could assume that if the most distal PEVK-actin attachment is knocked off at the beginning of the second shortening phase (Fig. 3, middle), all following PEVK-actin attachments of this particular titin molecule will also be knocked-off. Then, a factor decreasing from one towards zero with increasing velocity can simply be multiplied with the passive force in the second and the third shortening phases as well as with the length l_{block} of PEVK-inhibited binding sites to account for velocity-dependent force depression. Interestingly, the fraction of knocked-off PEVK-actin attachments might increase with a decreasing $f_{[break]}$. Thus, the current model yields the maximal force depression to be expected (Fig. 5), which may decrease with increasing velocities as stated in the literature, and moreover with decreasing $f_{[break]}$ (i.e. with increasing initial length or after an active pre-stretch).

During active isovelocity stretches, muscle stiffness was constant and greater than zero, independent of stretch velocity (Edman et al., 1982) and also independent of initial length (Till et al., 2008). The widely accepted product approach for the active force (Eq. (2)) leads to different active force slopes for different constant velocities in ranges of non-zero force-length relationship slopes, whereas the 'sticky-spring' mechanism in its current form yields passive forces which are independent of stretch velocity. Half-sarcomere force is the sum of active force and 'sticky-spring' force. Thus the experiments in the range of the plateau conducted by Edman et al. (1982) might be

explained, but those by Till et al. (2008) cannot be explained without accounting for a stretch-velocity dependence in the 'sticky-spring' mechanism model.

The increase in passive force attributed to increased titin stiffness in the presence of calcium was shown to be very small (e.g. Labeit et al., 2003; Joumaa et al., 2008) and would not be able to predict residual force enhancement values observed in experiments. However, Labeit et al. (2003) removed actin, and Joumaa et al. (2008) removed the tropomyosin motor troponin C. As a result, no myosin binding-sites on actin were available for the suggested PEVK-actin attachments which, in turn, are crucial for the 'sticky-spring' mechanism. However, the 'sticky-spring' forces depend on the force-elongation relations of distinct titin regions. Stiffness adaptations of these regions due to calcium increase may be worth considering, but were not accounted for in the model due to lack of data.

Functional implications

The proposed mechanism strongly links force enhancement with force depression effects, thereby implying functional consequences.

Passive, elastic force enhancement might improve the muscle's efficiency in cyclic stretch-shortening situations by temporarily storing and subsequently releasing elastic strain energy (Lindstedt et al., 2002; Pinniger et al., 2006). In a study with rats conducted by Lindstedt et al. (2002), eccentric muscle training increased muscle stiffness, but did not increase the rats' maximum isometric force, thus the ability of muscles to produce force enhancement (perhaps accompanied by force depression) seemed to be a plastic feature of muscles depending on their use. In this context, force depression could be seen as an unwanted by-product of force enhancement, and might be circumvented by timely deactivation in the shortening phase.

If the muscle's primary function is to produce positive work (i.e. active fiber shortening is the predominant action), the 'sticky-spring' mechanism is contra-indicated since by decreasing the muscle's force it leads to a reduction of the positive work. Muscle fibers and entire muscles showing no force enhancement exist (Pinniger et al., 2006; Stienen et al., 1992) and, following the proposed mechanism, they might lack force depression and might be adapted for production of positive work.

An intriguing aspect pointing to a possible source of the 'sticky-spring' mechanism's speculated adaptiveness might be the structural difference of heart titin when compared to skeletal muscle titin. The heart is one of the above mentioned muscles whose primary function is to produce positive work. The PEVK region in heart titin compared to that in selected skeletal muscles is very short (Linke et al., 1996), which is appropriate since it reduces the number of possible PEVK-actin connections and, therefore, reduces force depression.

Active shortening-stretch and stretch-shortening experiments

Non-commutativity of active shortening-stretch vs. stretch-shortening experiments with respect to the final steady-state force was found in experiments conducted by Herzog and Leonard (2000). Regarding the 'sticky-spring' mechanism, in such experiments the initial conditions for the second part of the experiment differ from single stretch or single shortening.

In an equidistant shortening-stretch experiment, shortening to an extent where the distal end of the attached PEVK region remains in place leads to equal configuration of the 'sticky-spring' at the final length compared to a purely isometric contraction at the same final length. Therefore, the steady-state force for both experiments may remain unchanged as reported (Herzog and Leonard, 2000). Greater shortening-stretch

amplitude can lead to the development of a force gradient in the PEVK region during stretch and, therefore, to force enhancement.

However, the situation for an equidistant stretch-shortening experiment of comparable amplitude would be different from the one already discussed. Due to stretch, the bound PEVK region elongates distally. During the first shortening phase, while the passive force decreases to zero, the force gradient in the PEVK region reverses with only marginal proximal displacement of the PEVK-region's distal end. Thus, the distal PEVK-region end is more distal when the final length is reached than it is in a purely isometric contraction at the same final length. As a result, the steady-state force at the final length is lower than the force resulting from the purely isometric contraction due to decreased passive force or even negative passive force and inhibited crossbridges (i.e. the 'sticky spring' introduces hysteresis).

The force decay after active stretch seen in experimental data

The force increase during active myofibril or muscle stretch can be separated into two main parts with different slopes. Pinniger et al. (2006) related the first part to increasing force-velocity values, and mainly associated the second part with increased titin stiffness. The force decay in a subsequent active isometric phase exceeds the force increase in the first part of the active stretch (e.g. Pinniger et al., 2006). This suggests that the force output of the 'sticky-spring' mechanism should decay in isometric conditions. It should be noted that this decay is incompatible with the 'sticky-spring' behavior as modeled.

Interestingly, it has been reported that, depending on force, the Ig regions unfold and refold in a statistical process (e.g. Linke and Grutzner, 2008). Assuming that the 'sticky-spring' mechanism is valid, force levels in the distal Ig region can vastly exceed those introduced by passive extension (Fig. 4) during and after active stretch. Therefore, the

456 unfolding of the distal Ig region might play a crucial role in the force decay after active
457 stretch. Accounting for such a process, the forces produced by the 'sticky-spring'
458 mechanism would inherit a velocity-dependence and force would decay in the isometric
459 phase after stretch.

460 Finally, in our model we did not account for increased passive titin stiffness due to
461 high calcium concentrations (Labeit et al., 2003) since to date it is not clear to what
462 extent which titin region stiffens. However, stiffening of mainly the distal Ig or the
463 PEVK regions, for example, might have a profound effect on 'sticky-spring' force
464 output during active stretch which, in turn, might lead to changed folding and unfolding
465 ratios and thereby influence overall time constant(s) of force decay.

466

467 **Acknowledgement**

468 We thank the German Science Foundation (DFG) for support of work (SI841/2-2).

469

470 APPENDIX A Calculation of f_l

471 We used the rat's actin length (1.04 μm; Walker and Schrodt, 1974), the typical
472 myosin length (1.6 μm), the measured plateau width (0.25 μm), and the measured
473 length of zero active force (1.27 μm) of the active sarcomere force-length relationship
474 (Gordon et al., 1966) to calculate the potential range of crossbridges l_{bind_pot} for a given
475 half-sarcomere length. The effective myosin bare-region length was assumed to
476 correspond to half the plateau width, thus the maximal range of operative crossbridges
477 $l_{[bind\_max]}$ per half-sarcomere is 1.6/2 – .25/4 = .7375 [μm]. In the range of the upper part
478 of the ascending limb, actin filaments entering the range of myosin heads of the
479 adjacent half-sarcomere are supposed to reduce the number of potential crossbridges by
480 half, thus the fraction of l_{bind_pot} in this range is halved. Subtraction of the length l_{block} of

PEVK-inhibited binding sites (compare Fig. 3) from l_{bind_pot}, and division by $l_{[bind\_max]}$ yielded the corresponding f_l value.

APPENDIX B Derivation of 'sticky-spring' stiffness during stretch

Consider a long active stretch of the activated half-sarcomere. The attached PEVK region elongates along actin and the force pulling on the distal PEVK region end increases due to 1) consecutive force bearing from distal to proximal PEVK segments in between initial PEVK-actin attachments and 2) superimposed force steps induced by binding sites approached during elongation.

Using the given passive force at any initial half-sarcomere length, we determined the initial PEVK-region length, $l_{PEVK[0]}$. Dividing $l_{PEVK[0]}$ by $c_{[bind]}$, the distance between two binding sites on actin (0.038 μm), and rounding up to the next integer yielded the number of initial PEVK-actin attachments. For simplicity, we assumed that the proximal end of the PEVK region would coincide with a PEVK-actin attachment. This led to full loading of all initial PEVK-actin attachments from the distal to the proximal end only when 'sticky-spring' force exceeded 2.5 $F_{[im]}$. Hence, the proximal Ig region did not elongate during stretch.

To calculate the 'sticky-spring' force-elongation relation (Fig. B.1A), we elongated the distal PEVK end by defined steps Δx_i and iterated the corresponding increased distal force f_i (Fig. B.1B). The length change Δl_k of the k-th recruited PEVK segment (i.e. PEVK segment loaded during active stretch) due to the segment-force increase from the force prior to the step $f_{i-1} - k\, f_{[am]}$ to the force after the step $f_i - k\, f_{[am]}$ is

$$\Delta l_k = c_{[bind]} \cdot \left(\frac{l_{PEVK}(f_i - k \cdot f_{[am]})}{l_{PEVK}(f_{i-1} - k \cdot f_{[am]})} - 1 \right). \qquad \text{(B.1)}$$

The expression in large parentheses yields the strain of the respective segment, which was calculated using the passive PEVK force-length relation (Fig. 2). Throughout appendices B and C, lengths depend on the forces written in parentheses. Each Δl_k migrates to the distal end and is finally strained by the force f_i. It is multiplied with a factor calculated again using the PEVK force-length relation to yield its final length. Δx_i is then expressed by

$$\Delta x_i = l_{end}(f_{i-1}) \cdot \left(\frac{l_{PEVK}(f_i)}{l_{PEVK}(f_{i-1})} - 1 \right) + \sum_{k=1}^{recr\_segs} \left(\Delta l_k \cdot \frac{l_{PEVK}(f_i)}{l_{PEVK}(f_i - k \cdot f_{[am]})} \right), \quad \text{(B.2)}$$

where the first term describes the elongation of the PEVK segment between the most distal PEVK-actin attachment and the PEVK-region's distal end with length $l_{end} < c_{[bind]}$. The *recr_segs* is the number of segments recruited for force-bearing by the 'sticky-spring' mechanism (Fig. B.1B).

Considering the thousands of titin molecules arranged in parallel in a sarcomere and the probability distribution of PEVK-actin attachment force, we approximated the 'sticky-spring' force increase to depend linearly on elongation (Fig. B.1A), resulting in a constant stiffness $k_{[sticky]}$ for each initial half-sarcomere length (Fig. B.1A, inset).

APPENDIX C The second active shortening phase

We calculated discontinuous force-shortening relations during the second shortening phase resulting from 'sticky-spring' peel-off for different initial sarcomere lengths (Fig. C.1A). For this purpose, we used the passive force-length relations of titin, the distal Ig region, and the PEVK region (Fig. 2). The free spring consists of the distal Ig region and a fraction of the PEVK region in series. Its length, l_{spring}, is expressed by

$$l_{spring} = l_{dist\_Ig}(f_{sticky}) + n \cdot c_{[bind]} \cdot \frac{l_{PEVK}(f_{sticky})}{l_{PEVK}(f_{pass[0]})}, \quad \text{(C.1)}$$

where n is the number of PEVK-actin attachments already broken. Force peaks occur due to the breaking of PEVK-actin attachments at $f_{[break]}$. The breaking of one distal PEVK-actin attachment induces a stepwise proximal displacement of the PEVK-region's distal end Δx_{PEVK_dist} (Fig. 3, middle) by $c_{[bind]}$. The half-sarcomere shortening distance from peak to peak $\Delta l_{[peak]}$ is expressed by

$$\Delta l_{[peak]} = c_{[bind]} \cdot \left(\frac{l_{PEVK}(f_{[break]})}{l_{PEVK}(f_{pass[0]})} + 1 \right). \quad \text{(C.2)}$$

Expected homogenization effects induced by the parallel arrangement of thousands of titin filaments with, for example, distributed PEVK-actin attachment strengths (Bianco et al, 2007), led us to translate the half-sarcomere length change to Δx_{PEVK_dist} via the gearing ratio $s(l_{hs[0]})$:

$$s(l_{hs[0]}) = \frac{c_{[bind]}}{\Delta l_{[peak]}} = \frac{l_{PEVK}(f_{pass[0]})}{l_{PEVK}(f_{pass[0]}) + l_{PEVK}(f_{[break]})}. \quad \text{(C.3)}$$

Integration of the discontinuous force-shortening relation (Fig. C.1A) yielded an approximately quadratic function (Fig. C.1B). To derive $l_{hs[0]}$-dependent $k_{[short\_2]}$, the constant stiffness related to second-phase half-sarcomere shortening $l_{hs[1]} - l_{hs}$ (Fig. C.1A, inset), we fitted $k_{[short\_2]} \cdot (l_{hs[1]} - l_{hs})^2 / 2$ to this function.

List of symbols and abbreviations

$c_{[bind]}$	distance of binding sites on actin (=.038 μm)
f_{act}	normalized active half-sarcomere force component
$F_{[am]}$	maximum bearable PEVK-actin attachment force (=8 pN)
$f_{[am]}$	normalized $F_{[am]}$ (= .16)
$f_{[break]}$	force in distal Ig region at which PEVK-actin attachment breaks (= $f_{[am]} - f_{pass[0]}$)
F_{hs}	half-sarcomere force
f_{hs}	normalized half-sarcomere force
$F_{[im]}$	maximum isometric force
f_l	factor due to active force-length relationship
f_{pass}	passive half-sarcomere force
$f_{pass[0]}$	initial passive half-sarcomere force
f_{sticky}	'sticky-spring' force (sum of forces pulling on the PEVK region)
$f_{sticky[2]}$	'sticky-spring' force at the end of the second shortening phase
f_v	factor due to active force-velocity relationship
$k_{[short\_2]}$	linear stiffness during second shortening phase
$k_{[sticky]}$	'sticky-spring' stiffness during stretch and during third phase shortening
l_{block}	length range with PEVK inhibited potential crossbridges
$l_{block[2]}$	length range with PEVK inhibited potential crossbridges at the end of the second shortening phase
l_{bind_pot}	potential range of operative crossbridges
$l_{[bind\_max]}$	maximal range of operative crossbridges
l_{dist_Ig}	length of titin's distal Ig region
$l_{dist\_Ig[0]}$	length of titin's distal Ig region attained under $f_{pass[0]}$
$l_{dist\_Ig[2]}$	length of titin's distal Ig region attained under $f_{sticky[2]}$

579	$l_{[dist\_Ig\_break]}$	length of titin's distal Ig region attained under $f_{[break]}$
580	l_{end}	length of PEVK region end in between most distal PEVK-actin
581		attachment and distal PEVK region end
582	l_{hs}	half-sarcomere length
583	$l_{hs[0]}$	half-sarcomere length at begin of first shortening phase
584	$l_{hs[1]}$	half-sarcomere length at begin of second shortening phase
585	$l_{hs[2]}$	half-sarcomere length at begin of third shortening phase
586	$l_{[myosin]}$	half myosin length (0.8 μm)
587	l_{PEVK}	length of titin's PEVK region
588	$l_{PEVK[0]}$	length of titin's PEVK region attained under $f_{pass[0]}$
589	n	number of initially bound PEVK segments
590	$recr\_segs$	number of PEVK segments recruited for 'sticky-spring' force bearing
591	s	slope of proximal PEVK end length change in second shortening phase
592	v_{hs}	half-sarcomere velocity
593	$x_{PEVK\_prox[0]}$	distance between Z-disc and proximal PEVK end at $l_{hs[0]}$
594	Δl_{dist_Ig}	length change of the distal Ig region
595	Δl_k	k-th recruited (loaded during active stretch) PEVK segment in between
596		PEVK-actin attachments (Fig. B.1B, bottom)
597	Δl_{sticky}	length change of the 'sticky spring'
598	Δx_i	defined elongation steps for determination of 'sticky spring' force-
599		elongation relation
600	Δx_{PEVK_dist}	length change of the distal PEVK end during shortening
601	Δx_{PEVK_prox}	length change of the proximal PEVK end during shortening
602		

References

Abbot, B.C., Aubert, X.M., 1952. The force exerted by active striated muscle during and after change of length. J. Physiol. 117, 77-86.

Bianco, P., Nagy, A., Kengyel, A., Szatmari, D., Martonfalvi, Z., Huber, T., Kellermayer, M.S., 2007. Interaction forces between F-actin and titin PEVK domain measured with optical tweezers. Biophys. J. 93, 2102-2109.

Bullimore, S.R., Leonard, T.R., Rassier, D.E., and Herzog, W., 2007. History-dependence of isometric muscle force: effect of prior stretch or shortening amplitude. J. Biomech. 40, 1518-1524.

Burkholder, T.J., Lieber, R.L., 2001. Sarcomere length operating range of vertebrate muscles during movement. J. Exp. Biol. 204, 1529-1536.

Edman, K.A., 1975. Mechanical deactivation induced by active shortening in isolated muscle fibres of the frog. J. Physiol. 246, 255-275.

Edman, K.A., 1996. Fatigue vs. shortening-induced deactivation in striated muscle. Acta Physiol. Scand. 156, 183-192.

Edman, K.A., Caputo, C., Lou, F., 1993. Depression of tetanic force induced by loaded shortening of frog muscle fibres. J. Physiol. 466, 535-552.

Edman, K.A., Elzinga, G., Noble, M.I., 1982. Residual force enhancement after stretch of contracting frog single muscle fibers. J. Gen. Physiol. 80, 769-784.

Forcinito, M., Epstein, M., Herzog, W., 1998. Can a rheological muscle model predict force depression/enhancement? J. Biomech. 31, 1093-1099., doi:10.1016/S0021-9290(98)00132-8.

Gordon, A.M., Huxley, A.F., Julian, F.J., 1966. The variation in isometric tension with sarcomere length in vertebrate muscle fibres. J. Physiol. 184, 170-192.

Herzog, W., Leonard, T.R., 1997. Depression of cat soleus-forces following isokinetic shortening. J. Biomech. 30, 865-872., doi:10.1016/S0021-9290(97)00046-8.

Herzog, W., Leonard, T.R., 2000. The history dependence of force production in mammalian skeletal muscle following stretch-shortening and shortening-stretch cycles. J. Biomech. 33, 531-542., doi:10.1016/S0021-9290(99)00221-3.

Herzog, W., Lee, E.J., Rassier, D.E., 2006. Residual force enhancement in skeletal muscle. J. Physiol. 574, 635-642.

Herzog, W., Leonard, T.R., Joumaa, V., Mehta, A., 2008. Mysteries of muscle contraction. J. Appl. Biomech. 24, 1-13.

Hill, A.V., 1938. The heat of shortening and the dynamic constants of muscle. Proc. Roy. Soc. Lond. 126, 136-195.

Huxley, A.F., Niedergerke, R., 1954. Structural changes in muscle during contraction; interference microscopy of living muscle fibres. Nature 173, 971-973.

Huxley, H., Hanson, J., 1954. Changes in the cross-striations of muscle during contraction and stretch and their structural interpretation. Nature 173, 973-976.

Huxley, A.F., 1957. Muscle structure and theories of contraction. Progr. Biophys. Chem. 7, 255-318.

Joumaa, V., Rassier, D.E., Leonard, T.R., and Herzog, W., 2008. The origin of passive force enhancement in skeletal muscle. Am J Physiol Cell Physiol 294, C74-8.

Kellermayer, M.S., Granzier, H.L., 1996. Calcium-dependent inhibition of in vitro thin-filament motility by native titin. FEBS Lett. 380, 281-286., doi:10.1016/0014-5793(96)00055-5.

Labeit, D., Watanabe, K., Witt, C., Fujita, H., Wu. Y., Lahmers, S., Funck, T., Labeit, S., Granzier, H., 2003. Calcium-dependent molecular spring elements in the giant protein titin. Proc. Natl. Acad. Sci. USA 100, 13716-13721.

Lee, E.J., Herzog, W., 2008. Residual force enhancement exceeds the isometric force at optimal sarcomere length for optimized stretch conditions. J. Appl. Physiol. 105, 457-462.

Lindstedt, S.L., Reich, T.E., Keim, P., LaStayo, P.C., 2002. Do muscles function as adaptable locomotor springs? J. Exp. Biol. 205, 2211-2216.

Linke, W.A., Ivemeyer, M., Olivieri, N., Kolmerer, B., Ruegg, J.C., Labeit, S., 1996. Towards a molecular understanding of the elasticity of titin. J. Mol. Biol. 261, 62-71., doi:10.1006/jmbi.1996.0441.

Linke, W.A., Grutzner A., 2008. Pulling single molecules of titin by AFM – recent advances and physiological implications. Pflugers Arch. 456, 101-115.

Linke, W.A., Ivemeyer, M., Mundel, P., Stockmeier, M.R., Kolmerer, B., 1998. Nature of PEVK-titin elasticity in skeletal muscle. Proc. Natl. Acad. Sci. USA 95, 8052-8057.

Marechal, G., Plaghki, L., 1979. The deficit of the isometric tetanic tension redeveloped after a release of frog muscle at a constant velocity. J. Gen. Physiol. 73, 453-467.

Meijer, K., Grootenboer, H.J., Koopman, H.F., van der Linden, B.J., Huijing, P.A., 1998. A Hill type model of rat medial gastrocnemius muscle that accounts for shortening history effects. J. Biomech. 31, 555-563., doi:10.1016/S0021-9290(98)00048-7.

Morgan, D.L, Mochon, S., Julian, F.J., 1982. A quantitative model of intersarcomere dynamics during fixed-end contractions of single frog muscle fibers. Biophys. J. 39, 189-196.

Morgan, D.L., 1990. New insights into the behavior of muscle during active lengthening. Biophys. J. 57, 209-221.

Morgan, D.L., Whitehead, N.P., Wise, A.K., Gregory, J.E., Proske, U., 2000. Tension changes in the cat soleus muscle following slow stretch or shortening of the contracting muscle. J. Physiol. 522, 503-513.

Niederlander, N., Raynaud, F., Astier, C., Chaussepied, P., 2004. Regulation of the actin-myosin interaction by titin. Eur. J. Biochem. 271, 4572-4581.

Peterson, D.R., Rassier, D.E., Herzog, W., 2004. Force enhancement in single skeletal muscle fibres on the ascending limb of the force-length relationship. J. Exp. Biol. 207, 2787-2791.

Pinniger, G.J., Ranatunga, K.W., Offer, G.W., 2006. Crossbridge and non-crossbridge contributions to tension in lengthening rat muscle: force-induced reversal of the power stroke. J. Physiol. 573, 627-643.

Prado, L.G., Makarenko, I., Andresen, C., Kruger, M., Opitz, C.A., Linke, W.A., 2005. Isoform diversity of giant proteins in relation to passive and active contractile properties of rabbit skeletal muscles. J. Gen. Physiol. 126, 461-480.

Stienen, G.J., Versteeg, P.G., Papp, Z., Elzinga, G., 1992. Mechanical properties of skinned rabbit psoas and soleus muscle fibres during lengthening: effects of phosphate and Ca2+. J. Physiol. 451, 503-523.

Sugi, H., Tsuchiya, T., 1988. Stiffness changes during enhancement and deficit of isometric force by slow length changes in frog skeletal muscle fibres. J. Physiol. 407, 215-229.

Till, O., Siebert, T., Rode, C., and Blickhan, R., 2008. Characterization of isovelocity extension of activated muscle: a Hill-type model for eccentric contractions and a method for parameter determination. J. Theor. Biol. 255, 176-187.

Walker, S.M., Schrodt, G.R., 1974. I segment lengths and thin filament periods in skeletal muscle fibers of the Rhesus monkey and the human. Anat. Rec. 178, 63-81.

FIGURE LEGENDS

Fig. 1. Schematic of the active (high calcium concentration) half-sarcomere: (top) at an initial length $l_{hs[0]}$ on the descending limb of the active force-length relationship; (middle) after stretch from $l_{hs[0]}$; (bottom) after shortening from $l_{hs[0]}$. All actin, myosin and titin (its molecular spring part is colored) filaments are represented with one specimen each. The long axis length ratios, as well as the number of myosin heads correspond to physiological values. (top) The PEVK region (yellow) is attached to actin at myosin binding sites (black dots). The length of titin's proximal Ig region, PEVK region, and distal Ig region attained under the initial passive force $f_{pass[0]}$ is depicted. (middle) The sum of the length changes Δl_{PEVK} and Δl_{dist_Ig} equals the stretch distance. (middle, enlarged view) The 'sticky-spring' force f_{sticky} equals the sum of attachment forces f_{att_i} pulling on the PEVK-actin attachments and $f_{pass[0]}$. (bottom) Inhibition of crossbridges by PEVK-actin attachments is illustrated.

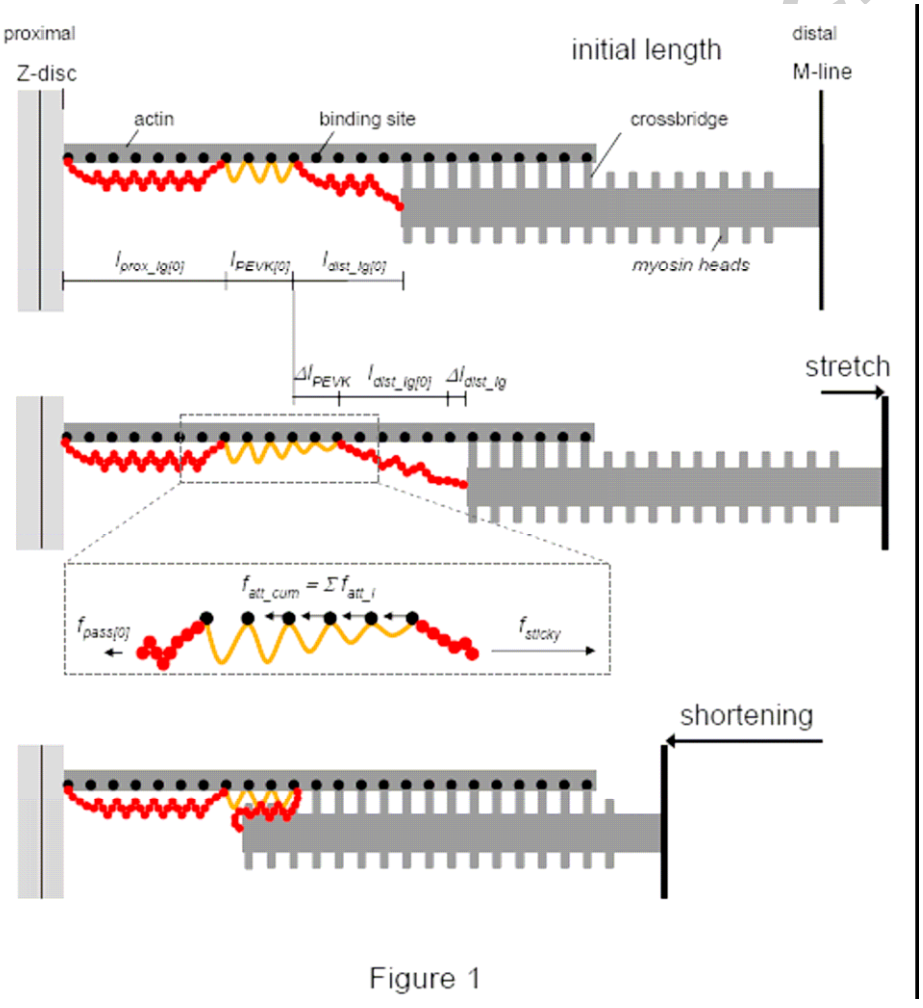

Figure 1

736 **Fig. 2.** Force-length relations (data adapted from Linke et al., 1998) of titin's entire molecular spring
737 region (x-mark), its PEVK region (square), and its distal Ig region (circle).

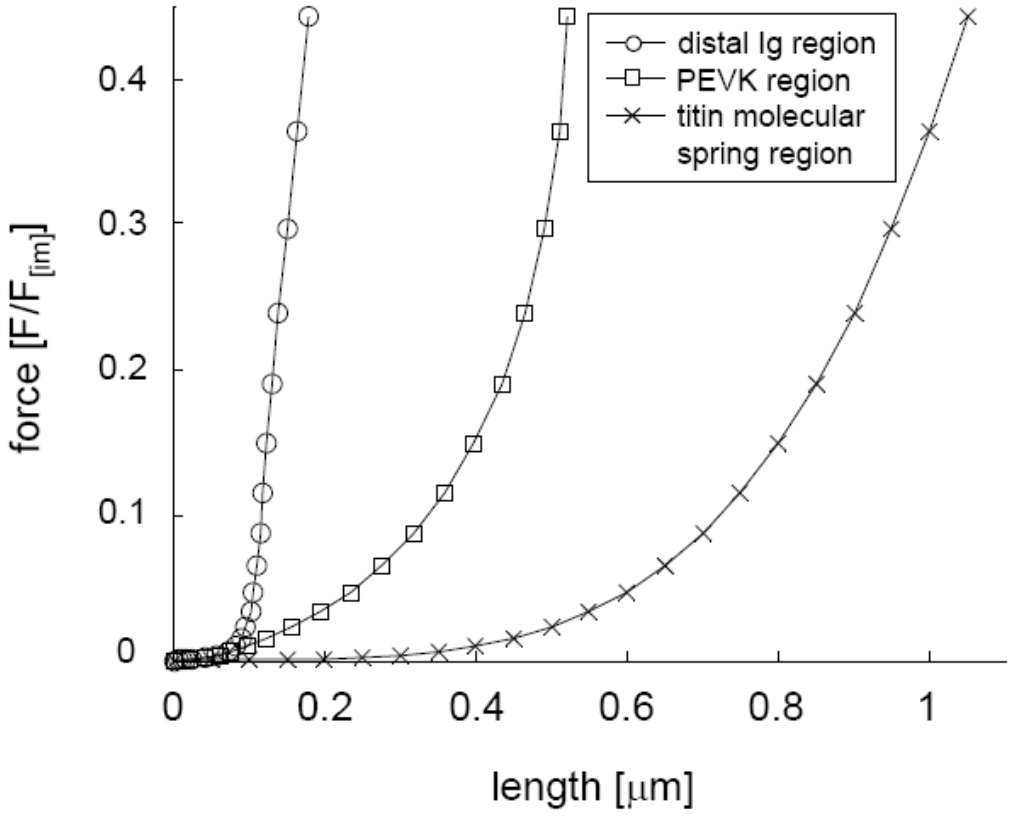

738 Figure 2

739

Fig. 3. Schematic of three subsequent phases (from top to bottom) of active half-sarcomere shortening. Only the vicinity of the myosin end and a part of the actin filament is depicted. The dark grey actin (dotted with binding sites) and myosin segments depict initial loci of the respective phase, and the transition between titin's PEVK region (yellow) and the distal Ig region (red) is marked with a circle containing a dot. The myosin segments depicted in light grey correspond to their position in a later stage, while the PEVK region and distal Ig region are now shown in grey. The arrows indicate length changes. (top) Shortening from the initial length results in quick unloading of the distal Ig region and proximal loading of the most distal PEVK actin attachment. (middle) The myosin end passes the distal end of the attached PEVK region and the attached PEVK region begins to peel off. Furthermore, dependent on the attached PEVK-region length and on the overlap with the myosin end, crossbridges are inhibited in the range l_{block}. (bottom) The sufficiently lengthened, peeled PEVK segment is allowed to reattach behind the attachment of its former proximal end. For further explanations see text.

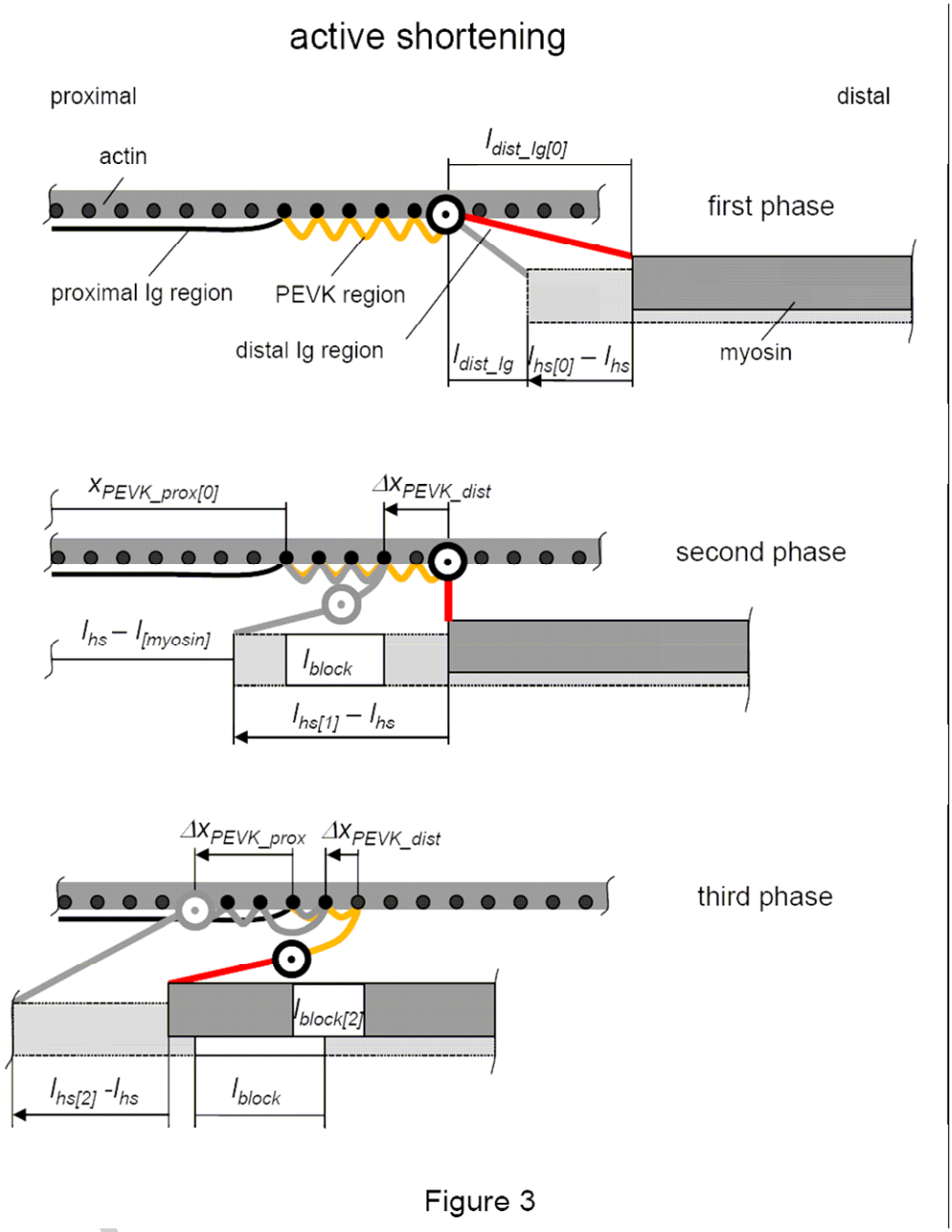

Figure 3

751

752

752 **Fig. 4.** Forces during quasi-isometric active stretch (thick lines). From top to bottom, the passive force,
753 the active force, and the sum of the two, the half-sarcomere force, is shown. For orientation, noted with
754 thin black lines, the passive (low calcium concentration) half-sarcomere force (top), the isometric active
755 half-sarcomere force (middle) and both as well as the sum of the two (bottom) are given.

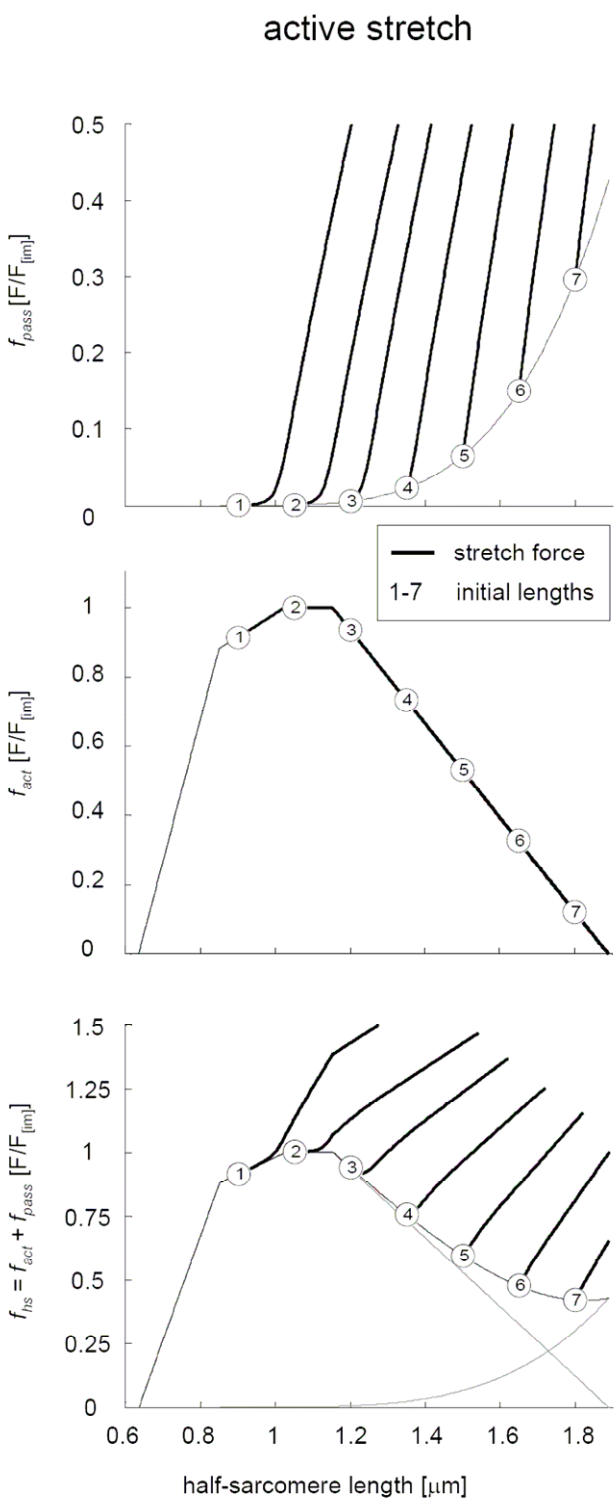

Figure 4

Fig. 5. Forces during quasi-isometric active shortening (thick lines). From top to bottom, the passive force, the active force and the sum of the two, the half-sarcomere force, is shown. The broken black line, the thick black line, and the thick grey line indicate the first, the second, and the third shortening phases, respectively. For orientation, noted with thin black lines, the passive (low calcium concentration) half-sarcomere force (top), the isometric active half-sarcomere force (middle), and both, as well as the sum of the two (bottom) are given. At the length .85μm, indicated by the vertical line, myosin hits the Z-disc.

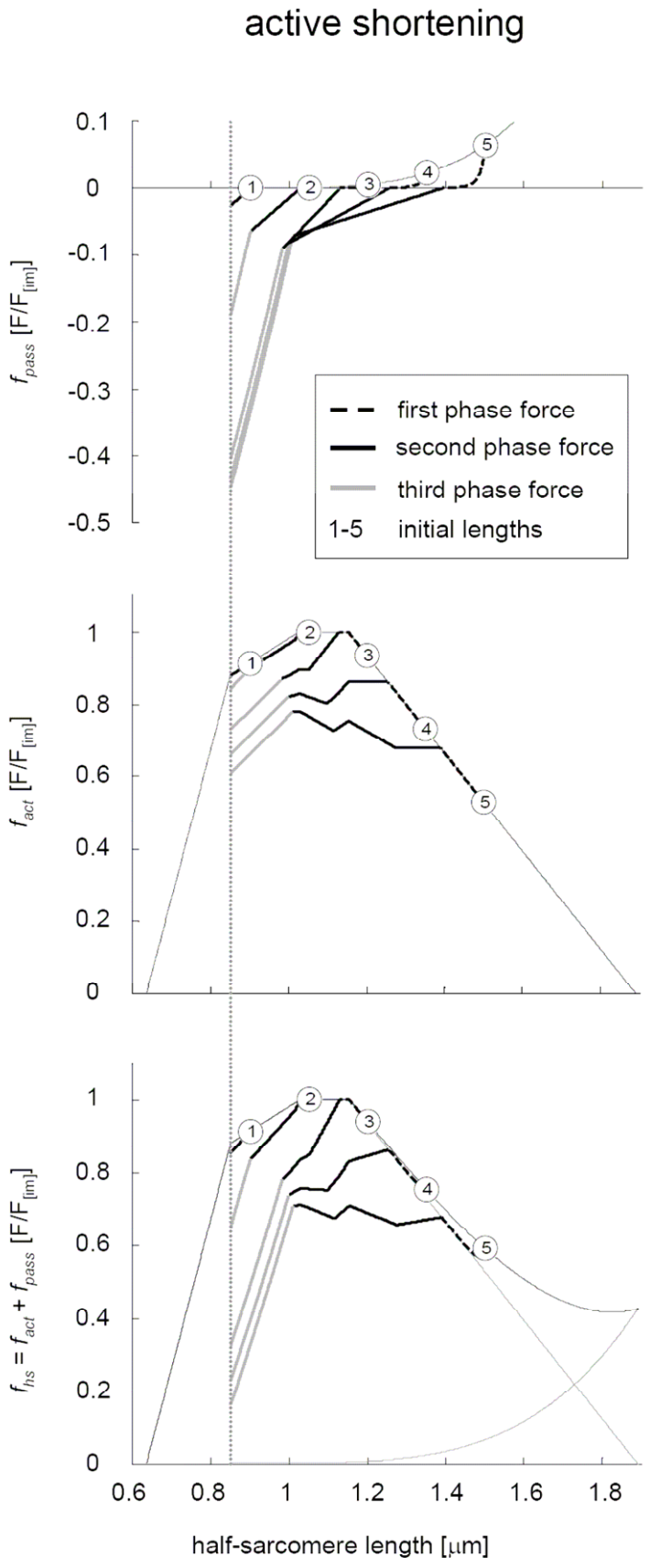

Figure 5

763

Fig. 6. Residual force depression (RFD). Thick lines show half-sarcomere forces due to quasi-isometric shortening from different (1-9) initial half-sarcomere lengths $l_{hs[0]}$. The vertical, broken line indicates a chosen, final half-sarcomere length. RFD (inset) depends almost linearly on the shortening distance (initial length – final length).

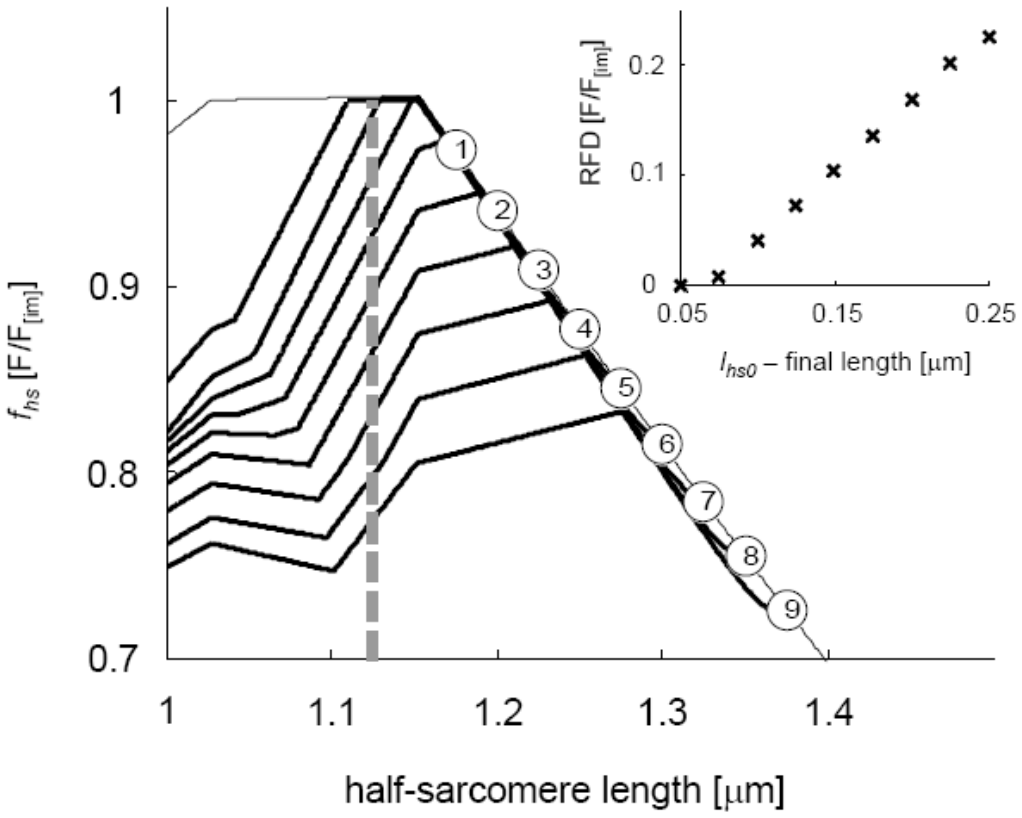

Figure 6

Fig. B.1. Linear approximation of 'sticky-spring' stiffness during stretch from different initial half-sarcomere lengths $l_{hs[0]}$. (A) Discontinuous force-elongation relations of the 'sticky-spring' resulting from stretch (black lines) are approximated linearly (grey lines). (A, inset) The linear 'sticky-spring' stiffness $k_{[sticky]}$ increases with increasing $l_{hs[0]}$. Circles correspond to the grey lines in A. (B) Schematic of 'sticky-spring' elongation by Δx_i. (B, top): The PEVK region is attached to actin. The distal Ig region and the PEVK segments 1 and 2 (encircled numbers) bear forces decreasing successively by the PEVK-actin attachment force $f_{[am]}$. The grey springs only bear the initial passive force $f_{pass[0]}$. (B, bottom) Stretch by Δx_i results in the same force increase in the distal PEVK-region end l_{end} and in segments 1 and 2. In this example, during stretch, the force difference between segments 2 and 3 exceeded $f_{[am]}$, and segment 3 now bears force exceeding $f_{pass[0]}$.

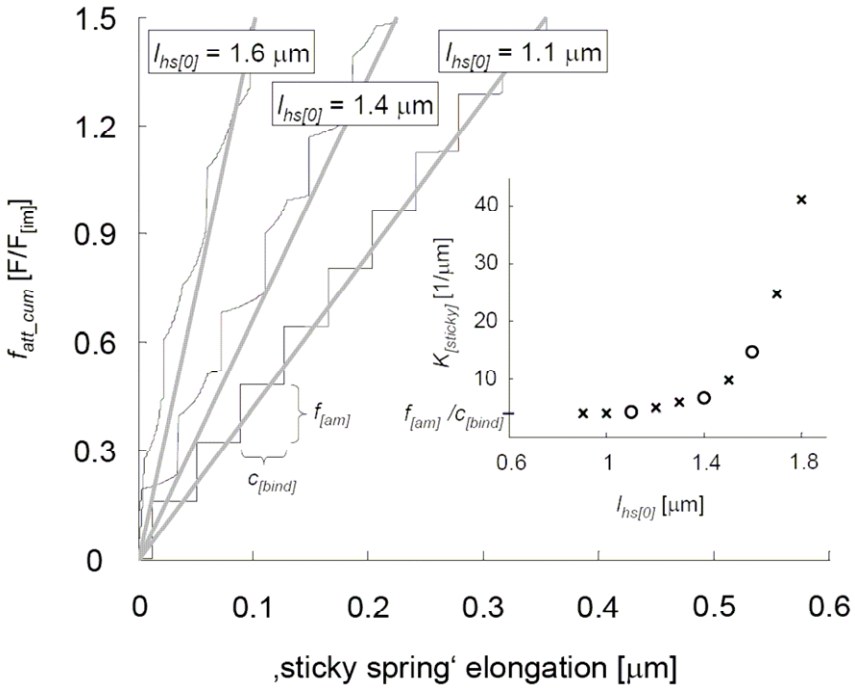

A

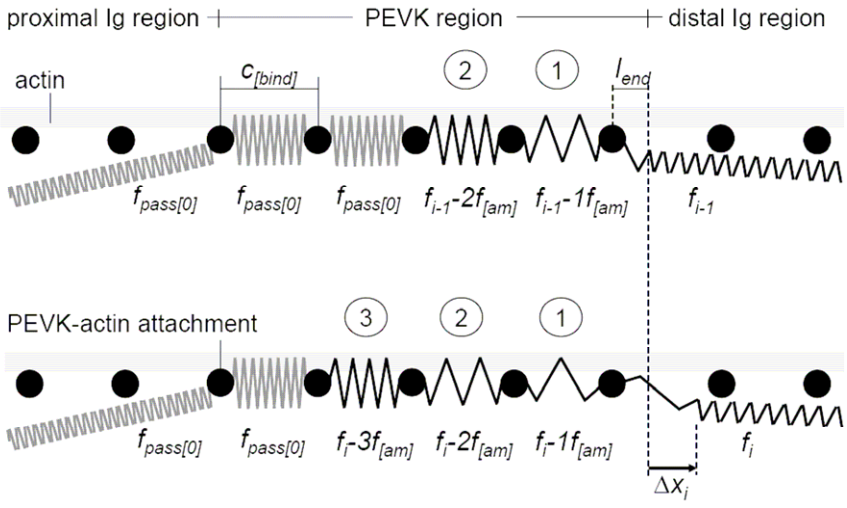

B

Figure B.1

779

780

Fig. C.1. Linear approximation of 'sticky-spring' peel-off force during the second shortening phase. (A) Discontinuous peel-off force dependent on selected initial half-sarcomere lengths $l_{hs[0]}$ plotted vs. second-phase half-sarcomere shortening $l_{hs1} - l_{hs}$. The corresponding approximate linear stiffness $k_{[short\_2]}$ depending on $l_{hs[0]}$ is shown in the inset (circles). The constant distance from peak to peak $\Delta l_{[peak]}$ is indicated for shortening from l_{hs0} = 1.6 µm. (B) According to the model, the mechanical energy (black lines) expended to peel off the PEVK region changes approximately with the square of the displacement similar to a linear spring. Parabolic approximation (grey lines) yields $k_{[short\_2]}$.

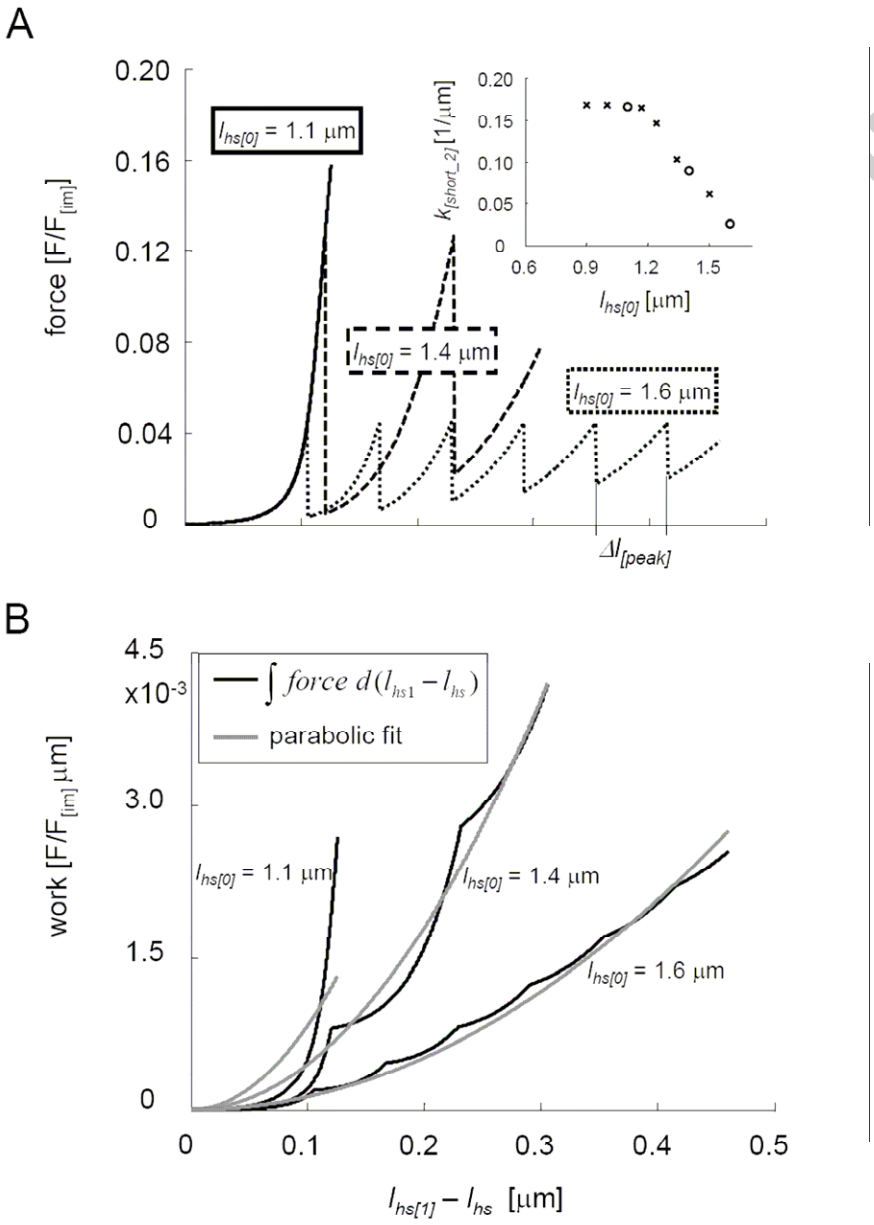

Figure C.1